

# Local Wettability Reversal during Steady-State Two-Phase Flow in Porous Media

Santanu Sinha,<sup>1,\*</sup> Morten Grøva,<sup>1</sup> Torgeir Bryge Ødegården,<sup>1</sup> Erik Skjetne,<sup>2</sup> and Alex Hansen<sup>1</sup>

<sup>1</sup>*Department of Physics, Norwegian University of Science and Technology, N-7491 Trondheim, Norway*

<sup>2</sup>*Statoil, Arkitekt Ebbellsvei 10, N-7005 Trondheim, Norway*

(Dated: February 7, 2012)

We study the effect of local wettability reversal on remobilizing immobile fluid clusters in steady-state two-phase flow in porous media. We consider a two dimensional network model for porous medium and introduce a wettability alteration mechanism. A qualitative change in the steady state flow patterns, destabilizing the percolating and trapped clusters, is observed as the system wettability is varied. When capillary forces are strong a finite wettability alteration is necessary to move the system from single-phase to two-phase flow regime. For the case of both phases being mobile we find a linear relationship between fractional flow and wettability alteration.

PACS numbers: 47.56.+r, 47.61.Jd

In a time of dwindling oil reserves, the fact that some 20 to 60 percent of the oil remains unrecovered at the end of oil production constitutes a challenge of increasing importance [1]. The reason for this loss is the formation of oil clusters embedded in water and held in place by capillary forces, which in turn are controlled by the wetting properties of the reservoir fluids with respect to the matrix rock. Therefore, the wetting properties of crude oil, brine and rock systems is a central research topic in the petroleum industry within the field of Enhanced Oil Recovery (EOR). EOR covers recovery methods other than pressure depletion (typical primary recovery) and water or gas injection (typical secondary recovery).

Formation wettability was reviewed recently in [2]. Reservoir rocks do not have uniform wetting properties. When a reservoir fluctuates spatially between strongly oil-wet and strongly water-wet it is called fractionally wet [3]. Sandstone is strongly water-wet before oil migrates from a source rock into the reservoir. After oil enters a pore it forms water films [4, 5] and a wettability alteration of the rock is believed to take place which can be irreversible due to direct adsorption of asphaltenes [6, 7] or can be reversible due to other surface active molecules present in the crude oil, such as carboxylic acids.

Both laboratory experiments and field tests have shown that deviation from strongly oil-wet to water-wet or neutral-wet conditions significantly increase oil recovery efficiency [8]. Wettability of reservoir rocks can be altered by changing the brine composition, e.g., lowering salinity [9], adding water-soluble surfactants [10] or even by adding oil-soluble organic acids or base [8]. An increase in temperature also increases water wetness of the reservoir [11]. Correlations have been shown with wetting behavior to the electrostatic forces between the mineral and oil surfaces [12]. Increasing the salinity level of the pore water makes the wetting transition shift in pH. The oil industry therefore paying a great attention towards low-salinity water flooding.

So far, there is no consensus on the dominating microscopic mechanisms behind the transport of the agent that

mediates the change in the pore wettability. The result of it, however, will be that there are correlations between the positions of the altered pores. In light of the massive uncertainty connected to the transport mechanisms, we simplify the problem assuming no correlation between positions of the altered pores. The precise question we pose in this paper is the following: Will the reversal of the wetting properties of a percentage of the pores lead to a significant change in the fractional flow patterns? We will see here that even without wettability switch correlations there can be a permanent change in fractional flow when the switched fraction of pores is large enough. How spatial correlations between the altered pores further affect the flow is a matter for future investigations.

In order to shed light on how local wettability alterations may remobilize stuck fluid clusters and to look for the consequences of this on the flow properties, we study here the effect of such alterations on a two-dimensional pore scale transport network model [13–15]. The mechanism for local wettability alteration is introduced in the model by changing the wetting contact angles of the menisci at pore necks. To study steady-state flow reflecting the situation deep inside the reservoir, we implement bi-periodic boundary conditions. The network is represented by a square lattice of cylindrical tubes, tilted  $45^\circ$  with respect to the imposed pressure gradient as well as the overall flow direction. Disorder is incorporated in the system by assigning the radius ( $r$ ) of each tube randomly from a flat distribution in the range  $[0.1l, 0.4l]$ , where  $l$  is the length of the tube. The network is filled with two immiscible fluids, named as water and oil, which flow inside the tubes (links). With respect to a pore, one fluid is less wetting while the other is more — hence there is a contact angle  $\theta$  associated with each meniscus. The tubes are cylindrical with respect to permeability, but they are considered hour-glass shaped with respect to the capillary pressure  $p_c$ . At position  $x$ ,  $p_c$  is obtained from a modified form of the Young-Laplace law [13, 16],

$$p_c = \frac{2\gamma \cos \theta}{r} \left[ 1 - \cos \frac{2\pi x}{l} \right], \quad (1)$$

where  $\gamma$  is the interfacial tension between the fluids. We define the wettability of the system by  $\omega = N_{\text{oil}}/N_{\text{total}}$ , where  $N_{\text{oil}}$  is the number of oil-wet links among the total  $N_{\text{total}}$  links in the system. Thus  $\omega = 0$  and  $\omega = 1$  represent pure water-wet and pure oil-wet systems respectively. A fractional value of  $\omega$  represents a fractionally wet system. When the wettability of a pore is altered, the direction of capillary forces at the menisci inside that pore changes. We therefore change the wettability of a pore in the model by altering the sign of  $p_c$ . In this work we consider a mixture of perfectly oil-wet and perfectly water-wet conditions, i.e.,  $\theta$  is either  $0^\circ$  or  $180^\circ$ .

The flow is driven by setting up an external global pressure drop. The local flow rate  $q$  in a tube with a pressure difference  $\Delta p$  between the two ends of that tube follows the Washburn equation of capillary flow [16, 17],

$$q = -\frac{ak}{\mu l}(\Delta p - \Sigma p_c), \quad (2)$$

where  $k$  is the permeability. For cylindrical tubes,  $k = r^2/8$  which is known from Hagen-Poiseuille flow. Here  $a$  is the cross-sectional area of the tube and  $\mu$  is the volume average of the viscosities of the phases present inside the tube. The sum over  $p_c$  runs over all menisci within the tube. The net flow at a node must be zero in a network. Eq. 2 then gives a large number of linear equations connecting the pressure variables at the nodes. The pressure field is obtained by solving the linear equations [18] and the flow field then follows from eq. 2. The system is forward time integrated by one step, using the explicit Euler scheme. Inside a tube all menisci move with a front speed determined from the local flow rate  $q$ , but when a meniscus reaches the end of a tube new menisci are formed in neighboring tubes maintaining the volume conservation. A maximum number of six menisci is considered here in a given tube. Further details of how the menisci are moved can be found in [14], though they are not necessary to understand the results of wettability alteration here.

The flow is controlled by the ratio between capillary and viscous forces at the pore level and quantified by capillary number  $\text{Ca} = \mu Q_{\text{tot}}/(\gamma \Sigma)$  where  $\Sigma$  is the cross-sectional area of the network and  $Q_{\text{tot}}$  is the total flow rate. Two different capillary numbers  $\text{Ca} = 1.0 \times 10^{-2}$  and  $\text{Ca} = 1.0 \times 10^{-3}$  are considered here. The ratio between the viscosities of the two fluids,  $M = \mu_o/\mu_w$  is another dimensionless parameter to control the flow, where  $\mu_o$  and  $\mu_w$  are the viscosities of oil and water respectively. Here we restrain our discussion to viscosity matched fluids which gives  $M = 1$ . Simulation is done considering a network of  $40 \times 40$  links. This is sufficiently large to be in the asymptotic limit for the range of parameters [14]. An average over 10 different samples has been taken for each simulation.

The simulation is performed under constant flow rate  $Q_{\text{tot}}$  which sets the capillary number. Initially, the sys-

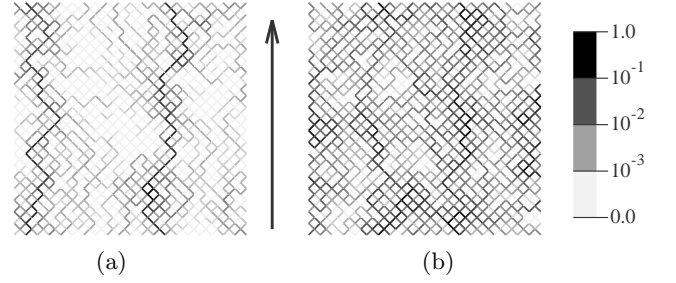


FIG. 1. Distribution of normalized local flow rates ( $q$ ) (a) before and (b) after the wettability alteration at  $\text{Ca} = 1.0 \times 10^{-3}$  and  $S = 0.6$ . The long arrow indicates the overall flow direction. The highest to lowest flow rates are indicated by darkest to lightest gray as shown by the scale. The steady state flow before wettability alteration is dominated inside only a few percolating paths as seen in (a). In (b), wettability of 50% tubes are altered and the percolating path breaks, causing the flow to be distributed over the whole network.

tem is pure water-wet ( $\omega = 0$ ) and filled with given oil and water saturations which remain constant throughout the simulation. Thus the saturation, capillary number and the wettability are the independent variables here. As the system evolves with time, it either starts a viscous fingering for high values of  $\text{Ca}$  or invasion percolation process when capillary forces dominate. Due to biperiodic boundary conditions, both drainage and imbibition take place simultaneously, leaving wetting and non-wetting fluid clusters in the system. On long timescales the system evolves to a steady state characterized by the system's macroscopic properties, such as global pressure, that becomes constant on the average. Mixing of two phases in steady state depends on the external control parameters, both  $\text{Ca}$  and the saturation of fluids. In Fig. 1(a), the distribution of normalized local flow rates at steady state is shown for the lower capillary number  $\text{Ca} = 1.0 \times 10^{-3}$ . If the difference in the saturation of the two fluids is large, one of the phases percolates the system with trapped immobile clusters of the other phase as can be seen in Fig. 1(a). Clearly, the flow is dominated through a few anisotropic percolating paths [19], leaving trapped immobile clusters in the system. In this case, we may apply Darcy's law for the single-phase pressure  $P_s$  along the system length  $L$  by,

$$\frac{Q}{\Sigma'} = \frac{k}{\mu} \frac{\Delta P_s}{L}, \quad (3)$$

which will be significantly larger than that of single-phase flow due to the smaller effective cross section  $\Sigma'$ . However, in the other situation when neither phase percolates the system and both the phases are mobile, all spanning flow paths contain interfaces associated with capillary forces. This situation requires even larger driving pressure due to the local dynamics of interfaces and capillary barriers. Therefore, as soon as low resistance percolating path appears in the system the global pressure drop de-

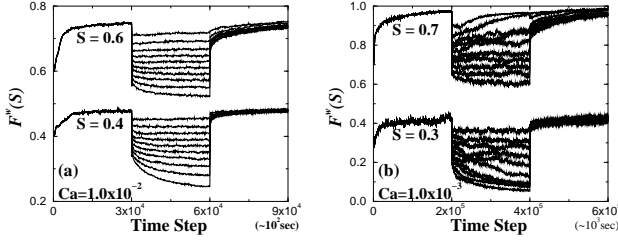


FIG. 2. Variation of oil fractional flow with time. Three different regions in each curve imply the time evolution in a water-wet system, then in a fractionally wet system after a wettability alteration  $\omega$  and finally restoring the initial water-wet system. For each saturation 10 different curves from top to bottom correspond to different values of  $\omega$  from 0.1 to 1.0 in intervals of 0.1. As  $\omega$  increases a gradual change in fractional flow is observed.

creases and the percolating and trapped clusters remain static. This is not favorable for oil-recovery purposes as it leaves immobile fluid in the reservoir.

After the system evolves to a steady state we change the wettability  $\omega$  by altering the direction of capillary forces in required number of links, chosen randomly. This initially perturbs the pressure field, deviates the system from existing steady state and subsequently leads it to settle into a new steady state. This again results to break any existing percolating and trapped fluid clusters which start flowing within a few time steps as illustrated in Fig. 1(b). If the wettability alteration is sufficiently large the change to a non-percolating system is permanent, otherwise new percolating cluster eventually appears.

We measure the fractional flow of oil, defined as the ratio between the flow of oil ( $Q_{oil}$ ) with the total flow ( $Q_{tot}$ ) as  $F^\omega(S) = Q_{oil}/Q_{tot}$  in a system with wettability  $\omega$  and oil saturation  $S$ . Independent simulations have been performed for different values of  $\omega$  and  $S$ . In Fig. 2,  $F^\omega(S)$  is plotted as a function of time. The three regions of the curves correspond to the initial pure water-wet ( $\omega = 0$ ) system, flipping wettability by a nonzero value of  $\omega$  and then again flipping them back to the initial  $\omega = 0$  value. There is a few things to notice. First, there is a gradual decrease in the steady state oil fractional flow with increasing  $\omega$ , i.e., more oil-wetness of the system. This is consistent with experimental results as it is observed that changing from oil-wet to mixed and water-wet systems, as in the case for low-salinity flooding, increases oil production [8, 10]. Secondly, the alteration process is reversible here, as in the third regime of the curves  $F^\omega(S)$  returns to the initial steady state value  $F^0(S)$ . Third, when the capillary forces are strong and the system is in a single-phase flow regime, a finite amount of wettability alteration is needed to move it towards a two-phase regime. This can be seen in Fig. 2(b), that for low capillary number  $Ca = 1.0 \times 10^{-3}$  and saturation  $S = 0.7$ , apart from an initial transient response, the steady state

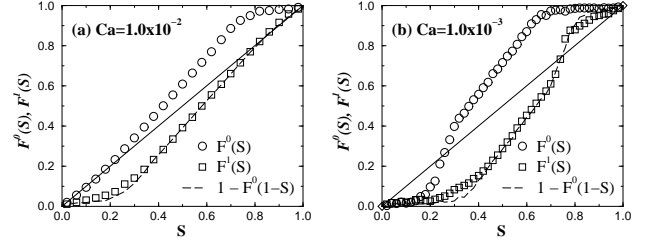


FIG. 3. Fractional flow as a function of saturation in water-wet ( $\circ$ ) and oil-wet ( $\square$ ) systems.  $1 - F^0(1 - S)$ , calculated from  $F^0(S)$ , is drawn by the dashed line which matches nicely with the  $F^1(S)$  curve.

fractional flow does not change for  $\omega \leq 0.2$ .

The variation of oil fractional flow with oil saturation  $S$  in a pure water-wet and a pure oil-wet systems are plotted in Fig. 3. In both the systems, the fractional flow does not follow  $F = S$  value represented by the solid straight line. This is due to the presence of interfaces with capillary pressure. The curves cross the  $F = S$  line from below at some point less than 50% saturation in pure water-wet and higher than 50% saturation in pure oil-wet systems. Fractional flow always higher in water-wet system ( $F^0(S)$ ) than in the oil-wet system ( $F^1(S)$ ). The difference  $\Delta F^1(S) = F^0(S) - F^1(S)$  depends on the saturation, it is zero at the two end points  $S = 0$  and 1. It is maximum in between, where both the phases are mobile. The maximum value of  $\Delta F$  increases with decreasing  $Ca$ , it is  $\approx 0.22$  for  $Ca = 1.0 \times 10^{-2}$  and  $\approx 0.40$  for  $Ca = 1.0 \times 10^{-3}$ . This due to the shape of the curves which strongly depend on  $Ca$  [20, 21].

As we consider only the case of viscosity ratio  $M = 1$ , a symmetric relationship between the fractional flow in pure water-wet and pure oil-wet systems is expected. From straight-forward symmetry argument we write the relation between the oil fractional flow in the two different systems as,

$$F^1(S) = 1 - F^0(1 - S). \quad (4)$$

In Fig. 3,  $1 - F^0(1 - S)$  is plotted by the dotted lines and it matches nicely with  $F^1(S)$  curve.

The wettability of real oil reservoirs generally have fractional wetting conditions. We therefore measure

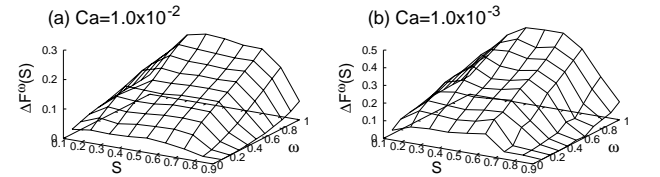


FIG. 4. Change in oil fractional flow  $\Delta F^\omega(S)$  with saturation and system wettability. For the lower capillary number, a finite  $\omega$  is required to have a non-zero value of  $\Delta F^\omega(S)$  at high saturations.

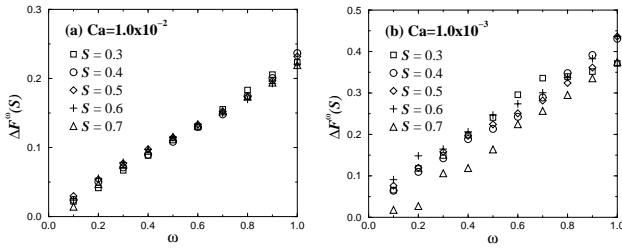


FIG. 5. Change in the oil fractional flow  $\Delta F^\omega(S)$  as a function of  $\omega$  at intermediate range of saturation, from  $S = 0.3$  to  $0.7$ . It can be seen that  $\Delta F^\omega(S)$  varies linearly with  $\omega$ .

$F^\omega(S)$  in different systems with fractional values of  $\omega$  from 0.1 to 1.0 in intervals of 0.1. The difference of  $F^\omega(S)$  from that in pure water-wet system,  $\Delta F^\omega(S) = F^0(S) - F^\omega(S)$ , is then calculated. In Fig. 4,  $\Delta F^\omega(S)$  is plotted as a function of saturation and wettability for the two different capillary numbers. It can be seen that the surface is more flat for the higher capillary number. Moreover, for the lower Ca there is a finite region with  $\Delta F^\omega(S) = 0$  to be noticed. It is already observed in Fig. 2(b) that for high saturation a finite wettability alteration  $\omega_{tr}$  is required to permanently change the system from a single-phase dominated regime. For  $\omega < \omega_{tr}$  we have  $\Delta F^\omega(S) = 0$ .

In order to find the functional dependence of  $\Delta F^\omega(S)$  on  $\omega$  in the regime where both the phases are mobile,  $\Delta F^\omega(S)$  is plotted against  $\omega$  in Fig. 5 for saturations from  $S = 0.3$  to  $0.7$ . The variation of  $\Delta F^\omega(S)$  with  $\omega$  is found to be linear here with some fluctuations. For  $\omega = 0$ ,  $\Delta F^0(S) = 0$ . For  $\omega = 1$ ,  $\Delta F^1(S)$  directly follows from Fig. 3 as the difference between the  $F^0(S)$  and  $F^1(S)$  curves. Assuming linearity in between, one can write

$$\Delta F^\omega(S) = \omega \Delta F^1(S) = \omega [F^0(S) - F^1(S)], \quad (5)$$

which we can combine with eq. 4 to obtain

$$F^\omega(S) = F^0(S) - \omega [F^0(S) + F^0(1 - S) - 1]. \quad (6)$$

This gives the functional dependence of fractional flow on both saturation and system wettability. It connects fractional flow in a *fractionally* wet system with that of a *purely* water-wet system by a linear relation with  $\omega$  and  $S$ . As fractional flow curves may be more easily obtained in samples of pure wetting properties, this equation may be useful to have an estimate of fractional flow when wettability is altered by, e.g., low-salinity water injection.

As  $\Delta F^1(S)$  is never negative it is clear that the fractional flow of oil will never decrease with the increase of water-wetness of the system. For a large viscosity contrast this result could vary, as our symmetry argument requires viscosity matched fluids. It is therefore requires further extensive numerical simulations to identify the results in that regime.

As a conclusion, we study the effect as well as the detailed pore level mechanism that causes the change in the steady state two-phase flow properties due to wettability alteration in porous media. A change in the system wettability causes a perturbation in the system's flow pattern to destabilize any percolating and trapped immobile clusters appeared in the steady state. In order to prevent forming similar structures again, a sufficiently strong wettability alteration is required depending upon the capillary number and saturation. When both the phases are mobile, fractional flow of oil is found to increase linearly with increasing water-wetness of the system. The results of our simulation are general in nature and consistent with the experimental results reported in literature qualitatively. They show that the remobilization of fluid clusters is due to purely fluid mechanical changes in the system induced by changes in the wetting contact angle — which in turn comes from the wettability alterations of the porous medium.

The authors thank Glenn Tørå for valuable discussions. The work has been financed through Norwegian Research Council (NFR) Grant No. 193298/S60.

\* Santanu.Sinha@ntnu.no

- [1] P. Roberts, *The end of oil: On the edge of a perilous new world* (Houghton Mifflin, New York, 2005).
- [2] W. Abdallah *et al.*, Schlumberger Oilfield Review **19**, 44 (2007).
- [3] M. J. Blunt, J. Pet. Sci. Eng. **20**, 117 (1998); J. S. Buckley, Curr. Opin. Coll. Int. Sci. **6**, 191 (2001); A. Skauge, K. Spildo, L. Høiland and B. Vik, J. Pet. Sci. Eng. **57**, 321 (2007).
- [4] J. Israelachvili, *Intermolecular and Surface Forces* (Academic Press, 3rd ed., 2011).
- [5] G. J. Hirasaki, in *Interfacial phenomena in petroleum recovery*, edited by N. R. Morrow (Marcell Dekker, New York, 1991), chs. 2 and 3.
- [6] A. R. Kovalscek, H. Wong, C. J. Radke, AIChE Journal, **39**, 1072 (1993).
- [7] R. Kaminsky, H. and C. J. Radke, Society of Petroleum Engineers, SPE 39087, 13 (1998).
- [8] M. T. Tveheyo, T. Holt and O. Torsæter, J. Pet. Sci. Eng. **24**, 179 (1999).
- [9] G. Q. Tang and N. R. Morrow, SPE Res. Eng. **12**, 269 (1997); J. Pet. Sci. Eng. **24**, 99 (1999).
- [10] D. C. Standnes and T. Austad, J. Pet. Sci. Eng. **28**, 123 (2000).
- [11] J. M. Schembre, G. Q. Tang and A. R. Kovalscek, J. Pet. Sci. Eng. **52**, 131 (2006).
- [12] J. S. Buckley, K. Takamura and N. R. Morrow, SPE Res. Eng. **4**, 332 (1989).
- [13] E. Aker, K. J. Måløy, A. Hansen and G. G. Batrouni, Transp. Porous Media **32**, 163 (1998); E. Aker, K. J. Måløy and A. Hansen, Phys. Rev. E **58**, 2217 (1998).
- [14] H. A. Knudsen, E. Aker and A. Hansen, Transp. Porous Media **47**, 99 (2002).
- [15] T. Ramstad and A. Hansen, Phys. Rev. E **73**, 026306

- (2006).
- [16] F. A. L. Dullien, *Porous Media: Fluid Transport and Pore Structure* (Academic Press, San Diego, 1992).
- [17] E. W. Washburn, Phys. Rev. **17**, 273 (1921).
- [18] G. G. Batrouni and A. Hansen, J. Stat. Phys. **52**, 747 (1988).
- [19] S. Sinha and S. B. Santra, Int. J. Mod. Phys. C **17**, 1285 (2006).
- [20] H. A. Knudsen and A. Hansen, Phys. Rev. E **65**, 056310 (2002).
- [21] H. A. Knudsen and A. Hansen, Eurphys. Lett. **65**, 200 (2004).